ce/papers Proceedings in civil engineering

Ernst & Sohn A Wiley Brand

ORIGINAL ARTICLE

ibausil
F. A. Finger-Institut für Baustoffkunde
Bauhaus-Universität Weimar

Efficient data generation for the determination of effective oxygen diffusion coefficients of cementitious materials

Viktor Kostic[1] | Alexander Haynack[1] | Jithender J. Timothy[1] | Thomas Kränkel[1]

Correspondence

Viktor Kostic
Technical University of Munich
Center for Building Materials
Franz-Langinger-Straße 10
81245 München
Email: viktor.kostic@tum.de

[1] Technical University of Munich, Germany; TUM School of Engineering and Design, Department of Materials Engineering, Center for Building Materials, Chair of Materials Science and Testing

Abstract

To develop new cementitious materials with the goal of reducing the carbon footprint a rapid assessment of information about their resistance against damaging processes is of utmost importance to ensure long-term durability. The Oxygen diffusion test is an efficient method to evaluate the ingress of gas in concretes and mortars without changing the porous structure of the specimen during testing. However, currently no standardized test method exists. We determined the effective Oxygen diffusion coefficient, $D_{e,O2}$ of mortar discs using a single diffusion cell method. Furthermore, we enhanced the procedure by extrapolating the oxygen saturation curves of the diffusion cells with a simple asymptotic function to identify a minimum required test duration where the extrapolated data still delivers reliable results and hence, shorten the overall required measurement time. In our case, we were able to significantly reduce the effort needed to obtain results that are within the range of the respective standard deviation of individual specimens. Our findings further strengthen the feasibility of time and cost efficient gas diffusion testing methods that could deliver complementary information for evaluating existing and designing new cementitious materials.

Keywords

Durability, Gas Diffusivity, Test Method, Service Life, Concentration

1 Introduction

Concrete structures are exposed to various potentially damaging environmental influences that can be a threat to their lifespan and durability. To ensure the target service life, currently a *prescriptive-based* design concept is used that ensures the durability requirements by specifying the material composition *(e.g., water/binder (w/b) ratio, binder type)* paired with the compressive strength. This, however, does not directly provide information about the porous structure of the hydrated cement matrix that characterizes the ingress of harmful substances. For example, high quality cements with high w/b-ratios satisfy the compressive strength requirements but have larger capillary pore fractions leading to increased available space for transportation processes [1].

The effective diffusion coefficient D_e is the intrinsic diffusivity of molecules in a reference medium corrected by the porosity and tortuosity of the given material. In general, the diffusion process is assumed to be governed by Fick's laws of diffusion [2]. Since effective diffusion coefficients are directly dependent on the material properties, it characterizes the resistance of the respective material against the ingress of potentially harming substances. Usually these coefficients are either estimated from models that account for the microstructural properties [3] or are obtained from experiments. [4–7].

Oxygen diffusion in cementitious materials is of interest due to several reasons: First, the presence of oxygen is necessary for corrosion of reinforcing steel in carbonated concretes [8]. Second, knowledge about gas diffusivity can contribute to further understanding of the carbonation process [9]. The diffusivity of carbon dioxide (CO_2) can be derived from measurements of the effective oxygen (O_2) diffusion coefficient $D_{e,O2}$ [5; 7; 8; 10] which circumvents the drawback of changes in the porous structure, caused by carbonation of the cement matrix during testing [11; 12].

To our knowledge, to this date no standardized method to evaluate the $D_{e,O2}$ of cementitious building materials exists. However, several methods have been developed (e.g. [7; 8; 13–15]). It is been shown that the oxygen diffusivity is directly associated with the porous structure and its distribution within the specimen [7], which itself is affected by the mixture design and the actual degree of carbonation [12]. Furthermore, the degree of moisture saturation drastically affect the diffusivity since water leads to clogging of the porous space needed for gas diffusion processes [7; 8; 16]. Thus, oxygen diffusion tests are a viable, non-destructive strategy for mortars and concretes to

assess information about their resistance towards gas ingress. However, a cost and time efficient as well as easy-to-handle standardized test method with minimal resources is yet to be finalized, since the above-mentioned methods still require elaborate test setups as well as personnel effort.

In the preliminary work of Boumaaza et al. [7; 9] a promising, straightforward setup was proposed, that analyzed the temporal oxygen concentration development $c_{O2}(t)$ in a single diffusion cell (see Figure 1 and 2). The concrete sample serves as a membrane between the diffusion cell and the adjacent atmosphere, commonly regulated climate chambers. To start the test, the cell is flushed with an inert gas (Nitrogen, N_2) to minimize its inner oxygen concentration. While the oxygen concentration inside the diffusion cell equalizes with the constant supply of ambient air through the specimen, $c_{O2}(t)$ inside the cell is measured (see Figure 2). Once equilibrium between the test environment and the diffusion cell is attained (steady state), $c_{O2}(t)$ can be used to calculate $D_{e,O2}$. This is achieved by minimizing the residual between the experimentally measured and the numerically computed $c_{O2}(t)$ obtained by solving Fick's second law of diffusion [2; 7; 17].

The rate of the gas diffusion process itself is known to be proportional to the square of the sample thickness [2], therefore leading to prolonged test times until a steady state is reached. Our reproductions of Boumaaza's oxygen diffusion test [7] with a specimen of 10 mm thickness, stored in 65 % relative humidity (RH) at 20 °C and atmospheric pressure took up to 10 days until the required $c_{O2}(t)$ to calculate $D_{e,O2}$ was measured. A temporally decreasing concentration gradient prolongs the oxygen accumulation process inside the diffusion cell gradually [2], increasing the time consumption. As shown in Figure 3, calculating the effective oxygen diffusion coefficient with the method proposed in [7] using only partially saturated diffusion cells with insufficient $c_{O2}(t)$ yields to strongly deviating results in the specimen diffusivity. Depending on the progression of $c_{O2}(t)$ in Figure 3, the results varied from 5.5e-05 (full-duration) to 9.2e-05 cm²/s (24 % of the full-duration test). However, since its progression is of asymptotic nature, we hypothesize that the measurement of $c_{O2}(t)$ can be partly circumvented. This is done by extrapolating the path of $c_{O2}(t)$ up until oxygen equilibrium is reached and therefore, shorten the overall test duration.

The goal of this study can be summarized as follows: enhancing the procedure following Boumaaza's oxygen diffusion test proposed in [7] to estimate the effective oxygen diffusion coefficient by extrapolating the rest of $c_{O2}(t)$ after certain intervals before the steady state is reached. A simple algorithm is used that fits sections of the recorded data series to an asymptotic function, generating extrapolated artificial datasets from the obtained parameters. Finally, to validate the reliability of the artificial saturation curves we use the approach of [7] as a basis to calculate the corresponding effective oxygen diffusion coefficients to compare the variance between the original as well as the extrapolated results by means of the progression of the initial monitored $c_{O2}(t)$. This contributes to a fast and efficient method of obtaining the information that is required to calculate effective oxygen diffusion coefficients of cementitious specimens for this specific setup.

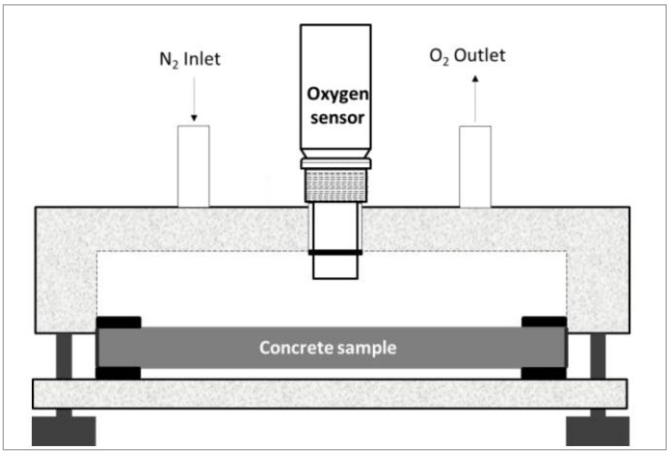

Figure 1 Cross-section of the setup used to measure $c_{O2}(t)$ [9]

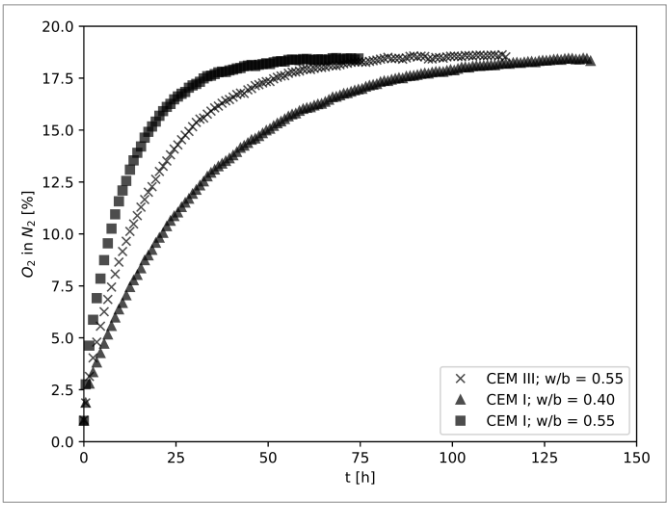

Figure 2 Temporal oxygen concentration development $c_{O2}(t)$ inside a diffusion cell with different specimen types of 10 mm thickness

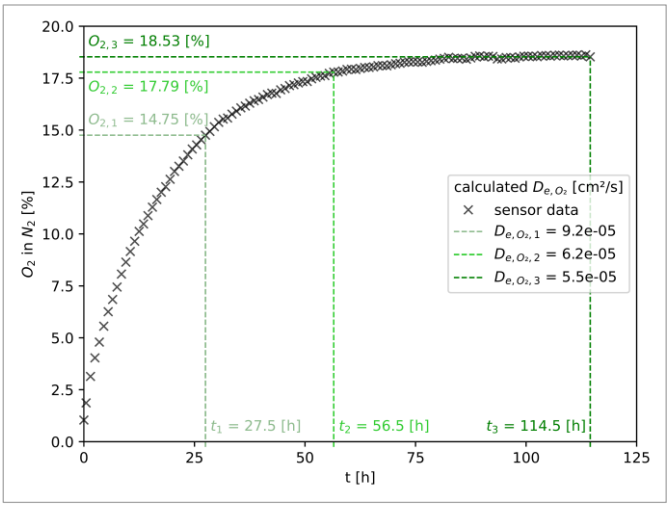

Figure 3 Three estimates of $D_{e,02}$ with Boumaaza's oxygen diffusion test [7] considering measured $c_{O2}(t)$ up to 27.5 h, 56.5 h and 114.5 h

2 Materials and methods

2.1 Materials

To develop a general approach to real-life application in the construction industry, we decided to produce mortar discs of 10 mm thickness with a diameter of 100 mm.

These dimensions were chosen for several reasons: First, mortar or concrete discs of 10 mm can easily be sawn from extracted cores of building sites or prepared in laboratories. Second, the attachment to the diffusion cell turned out to be easier with round-shaped specimens and therefore reduced the risk of leakages.

To generate a targeted variation in the expected effective oxygen diffusion coefficients and thus the required testing times we used ordinary Portland cement (OPC) and slag-blended cement (*CEM I 42,5 N* and *CEM III/B 42.5 N–LH/SR* according to EN 197-1 [18]) with w/b ratios of 0.40 and 0.55. The maximum grain size of the aggregates was 2 mm. It was kept constant for all mortar mixtures. An overview of the mixture designs is given in Table 1. We produced a series of three specimens for every mixture M1-M4 following EN 197-1 [18].

Table 1 Mortar mix designs

Mixture	M1	M2	M3	M4
CEM	I	I	III/B	III/B
w/b	0.40	0.55	0.40	0.55
Cement kg/m³	680	560	665	550
Water kg/m³	272	308	266	302.5
Aggregates kg/m³	1,307	1,312	1,310	1,315

All samples were cured identically as follows: immediately after casting, the specimens were stored in 100 % RH for two days before being demolded and cured by storage in water until a mortar age of seven days. Afterwards curing continued in a climate chamber at 20 °C, 65 % RH) until the age of 28 days. Subsequently, all samples were oven dried at 50 °C for four days to stop the hydration process and by doing so to avoid changes in the cement matrix during the diffusivity measurements. After oven drying we further preconditioned the samples by storing them again at 20 °C and 65 % RH until the age of 56 days. To ensure one-dimensional diffusion, the lateral surfaces of the discs were sealed with aluminum-laminated butyl-tape beforehand.

2.2 Effective diffusion coefficient measurement

The method of evaluating the effective oxygen diffusion coefficients $D_{e,O2}$ of mortars in this contribution relies on the previous work of Boumaaza et al., which is described in detail in [7] and [9]. This method was chosen due to its straightforward nature of creating a temporal oxygen concentration development ($c_{O2}(t)$) dataset with easy reproducibility and reliability in results [7; 9; 12; 19].

A single diffusion cell is used to create an oxygen concentration gradient between the internal cell volume and the ambient air of a regulated climate chamber (20 °C, 65 % RH) (see Figure 1). After connecting the samples to the bottom opening of the cell with silicone and aluminum-laminated butyl-tape, the inner chamber is flushed through the inlet opening with N_2 to decrease the inner O_2 concentration to ~0.5 %. Subsequently O_2 starts to diffuse through the sample until equilibrium is reestablished. Since the volume of the climate chamber is more than 10^3 times higher than the diffusion cell capacity (300 cm³) a constant supply of oxygen can be assumed [9]. A sensor (*Vernier Go Direct ® O_2 Sensor*) is monitoring $c_{O2}(t)$ as the concentration of O_2 in N_2 inside the cell every 20 seconds (see Figure 4). We later smoothened the data by averaging the oxygen content within a time period of one hour. For the calculation of the effective oxygen diffusion coefficient based on Fick's second law of diffusion, the equilibrium state in terms of oxygen percentage between the climate chamber and diffusion cell has to be reached [2; 7]. Due to the asymptotic behaviour this can be recognized as a visible plateau in the sensor data (see Figure 4). Alternatively, a prior measurement of the maximum oxygen percentage of the test environment can be done. By curve-fitting of the experimental data with a python program to a solution of Fick's model, the diffusion coefficient can be determined. A detailed description is to be found in [7] and [17]. Every mixture series of the specimen was tested concurrently in the same climate conditions where the preconditioning has been conducted. Once the equilibrium was reached, the measurements were stopped simultaneously; however, since it is almost impossible to start at exactly the same oxygen percentages for all single specimens, we decided to cut the starting point of the data to 1.0 % to ensure same conditions for every calculation.

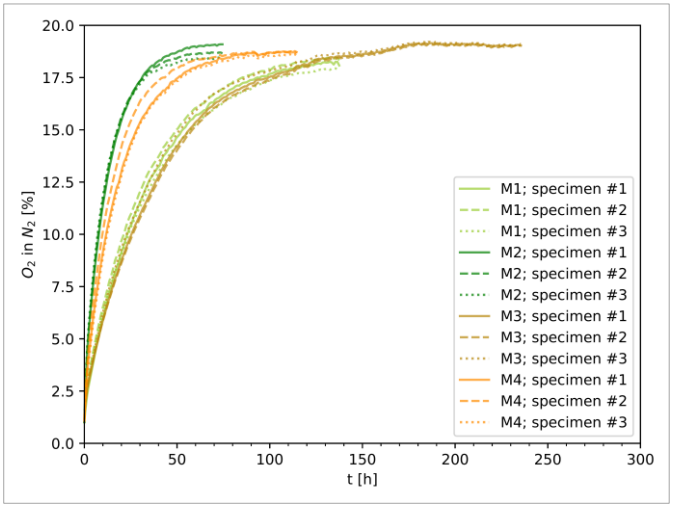

Figure 4 Monitoring the development of $c_{O2}(t)$ inside the diffusion cell; three specimen of every mixture were tested simultaneously

2.3 Extrapolation algorithm

The output of this measuring method is the temporal oxygen concentration development $c_{O2}(t)$ inside the diffusion cell. As expected, all of our full-duration datasets followed an asymptotic course, see Figure 4. To extrapolate $c_{O2}(t)$ using limited measurement data before reaching equilibrium, a suitable function is needed. Therefore, we used the equations of the *External Influence Model (EIM)* from the field of Information Diffusion in Online Social Networks [20]:

$$c_i = c_{eq} - \left(c_{eq} - c_{start}\right) * e^{(-k * t_i)} \qquad (1)$$

The O_2 in N_2 percentage c_i [%] at a given time t_i [h] in

equation (1) is dependent on the steady-state oxygen concentration c_{eq} [%] reached at equilibrium, its initial oxygen concentration c_{start} [%] at $t_i = 0$ [h] and the parameter k [1/h]. The latter variable k defines the curvature of $c_{O2}(t)$ and is linked to the material properties and its surroundings, hence the speed of the diffusion process [20]. It can be acquired by curve-fitting of the experimental data with a function of the Python SciPy library [21]. This function uses the non-linear least squares method to determine k of equation (1). Figure 5 shows exemplary curve-fits of the measured full-duration $c_{O2}(t)$ data of single specimens within the mixture series combined with their resulting mean squared errors *MSE*. Note that for the development of this extrapolation method the measurement of each individual specimen is taken into account separately. This ensures the suitability of this method for the evaluation of varying $c_{O2}(t)$ developments, hence different material compositions. Table 2 gives an overview of every corresponding *MSE* of the specimens that were tested within the scope of this paper. The low *MSE* indicate a low divergence between the experimental data and equation (1), further enhancing the suitability of this function.

Table 2 Resulting mean squared errors (MSE) of curve-fitting the measured full-duration $c_{O2}(t)$ data to equation (1)

Mixture	M1	M2	M3	M4
MSE specimen #1	0.0498	0.0960	0.0443	0.0518
MSE specimen #2	0.0655	0.0697	0.0616	0.0527
MSE specimen #3	0.0823	0.1067	0.0455	0.0325

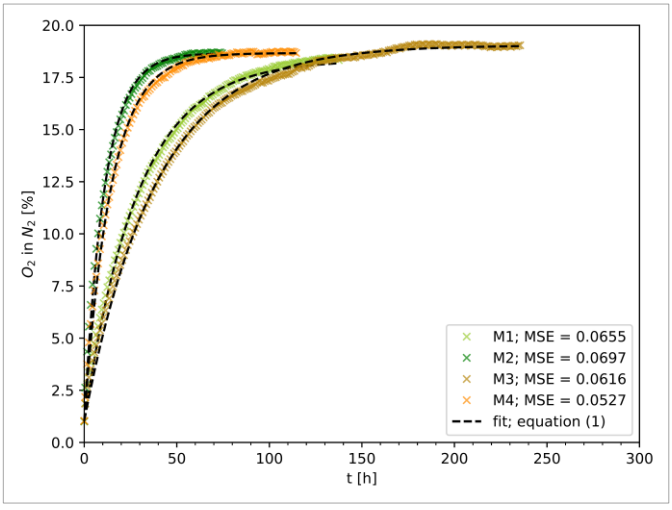

Figure 5 Exemplary curve-fitting the measured full-duration $c_{O2}(t)$ data of single specimens within the mixture series to equation (1) (dashed line) as well as their corresponding mean squared errors (MSE)

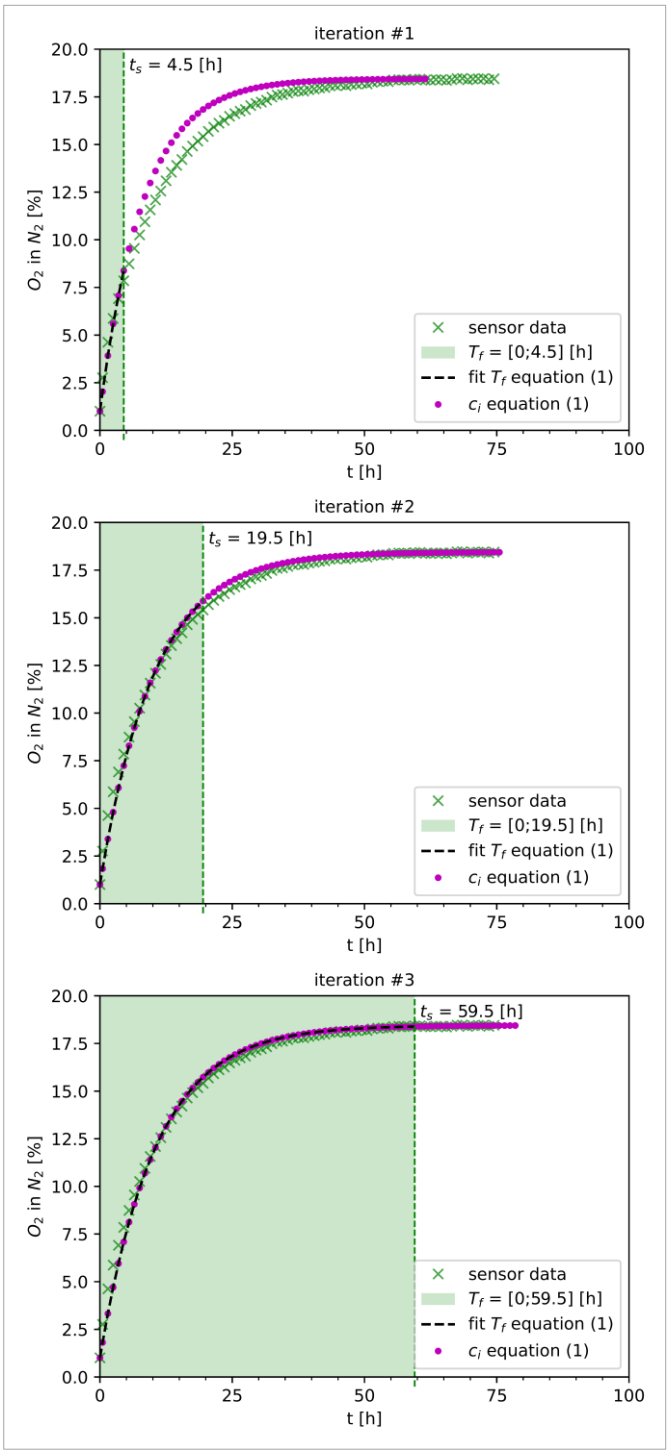

Figure 6 Exemplary section-wise extrapolation iterations of initial sensor data (74.5 h); the green area (timeframe T_f) illustrates the amount of data that was used to generate the artificial values c_i with equations (1-4) and inputs of $c_{start} = 1.0$; $c_{eq} = 18.45$ in terms of % O_2 in N_2

Dividing the datasets into different intervals T_f [h] (equation (2)) and using their corresponding k_{T_f} allows to extrapolate the development of $c_{O2}(t)$ using equation (1), see Figure 6.

$$T_f = [t_0; t_s] \tag{2}$$

Note that the determination of c_{start} and c_{eq} is crucial for this implementation. However, c_{start} can be set as the initial measurement value and c_{eq} can easily be obtained by prior monitoring of the test environment. In this study we

defined c_{eq} as the last value in our full-duration datasets, c_{start} was set to 1.0 %. Furthermore, a certain timespan for the extrapolated curve has to be specified. Without the full-duration datasets we cannot know the exact length of a single test, however we can approximate the duration by simply setting c_i to a concentration 0.01 % below c_{eq}. This allows us to rearrange equation (1) to solve for the expected time t_{eq} until equilibrium for the k_{t_s} (equation (4)) to reach the condition in equation (3):

$$c_i = c_{eq} - 0.01 \tag{3}$$

$$t_{eq} = \frac{ln(c_{eq} - c_{start}) - ln(0.01)}{k_{T_f}} \tag{4}$$

The generated extrapolated datasets of $c_{O2}(t)$ as shown in Figure 6 can then be evaluated by Boumaaza's oxygen diffusion test method according to [7; 9] to calculate the effective oxygen diffusion coefficient of the corresponding specimen. Contrary to the natural diffusion process, the addition of this algorithm enables the possibility to shorten the required evaluation time and thus enhance the overall efficiency of the test.

3 Results

The results are separated in two parts. At first, the evaluation of the full-duration datasets of $c_{O2}(t)$ according to Boumaaza's oxygen diffusion test proposed in [7]. Second, comparing the results with those of the extrapolated datasets as a function of the used test duration t_s.

Table 3 shows the average effective diffusion coefficients of three related full-duration tests accompanied by their time requirement to reach oxygen equilibrium. Generally, a higher w/b-ratio seems to lead to higher effective diffusion coefficients within the same binder type. Also, the specimen with slag blended cements show a decrease in their coefficients in comparison to their OPC counterparts within the same w/b-ratio.

Table 3 Average oxygen diffusion coefficients of the mortar discs

Mixture	w/b	$D_{e,O2}$ *cm²/s*	std. dev. *cm²/s*	duration *h*
M1	0.40	3.19e-05	1.09e-06	138
M2	0.55	8.95e-05	5.19e-06	75
M3	0.40	2.61e-05	1.30e-06	236
M4	0.55	5.96e-05	6.20e-06	115

In order to evaluate our algorithm we sectioned the original full-duration data of $c_{O2}(t)$ by cumulatively increasing t_s, adding three hours of data each iteration before extrapolation. Figure 7 shows the progressive change of the resulting artificial $D_{e,O2,s}$ as a function of t_s. Note that we chose to combine the results of different mixtures into single subplots to improve the visibility. Each subplot of Figure 7 shows the individual results of one out of three specimens for every mixture series (M1-M4). The coloured solid lines represent the original coefficients $D_{e,O2,org}$ resulting from the single full-duration measurements. To define a threshold, we used the corresponding standard deviation of each mixture series: values within this boundary indicate a deviation between the experimental and artificial results that is comparable to the natural error within the specimen. All of the tests approach this barrier earlier than the initially required time and therefore, generated eligible results without having access to the full-duration datasets of $c_{O2}(t)$.

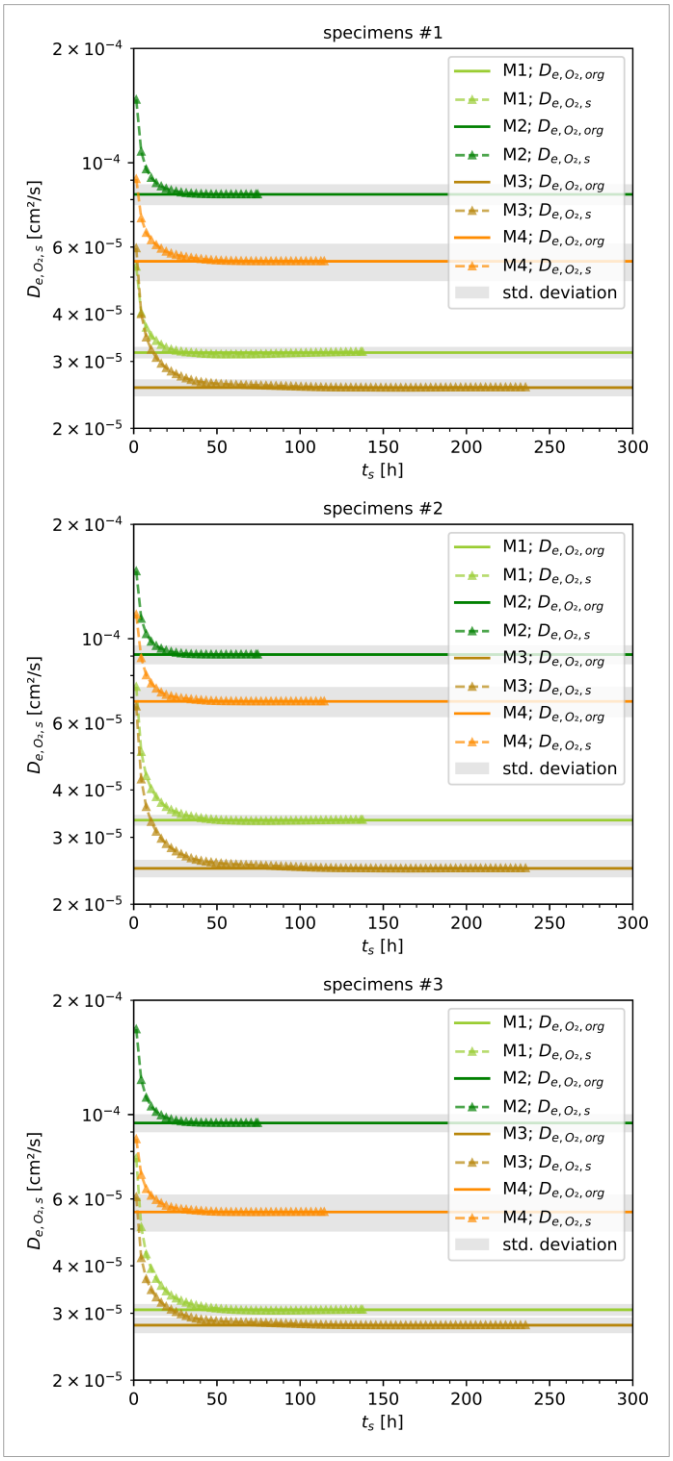

Figure 7 Progression of the artificial $D_{e,O2,s}$ of each individual specimen within the mixture series as a function of the used testing time t_s; solid lines indicate the original results $D_{e,O2,org}$ with their respective standard deviation depicted as grey area

4 Discussion

Our results are in accordance with literature by showing the deviating effects of different binder types or w/b-ratios on the effective oxygen diffusion coefficients of the samples. It is stated that this behavior can be attributed to the development of different porous structures and varying pore size distribution during the hydration process [5; 8; 10; 12; 22]. However, we did not conduct any examination of the specimen in this manner. Nevertheless, a clear decrease in the magnitude of $D_{e,O2}$ for decreasing w/b from 0.55 to 0.40 can be recognized within both mixtures, which could be the consequence of a smaller volume of capillary pores, thus providing less space for gas diffusion processes [7; 8]. Previous studies [5; 12] indicate that in comparison to OPC, the pore size distribution of hardened slag-blended cements like CEM III/B is shifted towards finer pores. We also assume this phenomenon to be responsible for the slight change in the resulting $D_{e,O2}$ between the two binder types with equal w/b-ratios. Furthermore, the acquired values are in a comparable range as those of concrete specimen in [9] (9.5e-04 – 2.1e-05 cm²/s). However, note that those rely on different boundary conditions and concrete designs, hence can only be compared in a qualitative manner.

The extrapolation of artificial datasets by using only sections of the full-duration datasets of $c_{O2}(t)$ introduces the opportunity to significantly decrease the time requirement to estimate the effective oxygen diffusion coefficient of cementitious materials. The deviation between the experimental $D_{e,O2,org}$ and extrapolated $D_{e,O2,s}$ is dependent on the considered test time t_s. of the full-duration $c_{O2}(t)$ measurements (see Figure 7). In this study, we used the standard deviation as a reference since within that margin our mixtures are still distinguishable and hence eligible for a qualitative comparison. Due to the rather small experimental data obtained from three specimens per mixture, it is not possible to pinpoint an exact value. However, stopping after 10-30 % total test time duration until equilibrium seems to be sufficient to reach values within the standard deviation of the corresponding specimens. Cementitious materials are composed of heterogeneous structures that form rather randomly [23]. Therefore, the observation of transport processes between specimens of the same type will always result in a specific variation [1]. This phenomenon makes small errors in exchange of time efficiency more acceptable. To fulfil the needs for precision in future implementations a specific error-threshold must be further investigated. In addition, it must be noted that we had knowledge of all parameters regarding the minimum and maximum values of oxygen percentage, though these could be easily determined by prior measurements of the test environment. Since the asymptotic equation (1) in our method is a simple mathematical term that does not directly relate to the actual gas diffusion process in porous media, we suggest that there could be more optimized ways to extrapolate the data and minimize the error between the experimental and extrapolated data. Further investigations could lead to a more specialized algorithm that regards specific specimen and binder types, thicknesses, or climate conditions. However, this is beyond the scope of this study. We also hypothesize that this method could as well be used for the temporal asymptotic concentration development of other inert gases or substances.

5 Conclusion

Within the scope of this research, an extrapolation method was proposed that shows the possibility to significantly shorten the time investment to acquire the necessary data for the evaluation of oxygen diffusivity of cementitious building materials. This was done by aborting the measurement of the temporal oxygen concentration development $c_{O2}(t)$ after certain time-intervals and extrapolating the remaining data until steady state. To analyze the results from our extrapolated data we used an existing single-cell diffusion method that relies on $c_{O2}(t)$ to obtain the effective oxygen diffusion coefficients of mortars. Despite a slightly higher error margin compared to the natural full-duration tests depending on the progression of the original data, we consider our method as a viable enhancement to lower the efforts and costs in this particular setup. In our case, the required duration to gather the necessary information to reach results within the specimens' standard deviation could be reduced significantly. Furthermore, it is hypothesized that this method can also be transferred to predict the temporal asymptotic concentration development for different inert substances. To consolidate this, a broader spectrum of concrete mixtures as well as optimization of the extrapolation function must be done. Nevertheless, to a certain extent these findings further pave the way for generalized future testing methods that allow a more precise and cost-efficient method for estimating the durability of concrete structures that outperform the existing concepts.

Acknowledgement

This work has been supported by the German Research Foundation (DFG), project number 428338963. This support is gratefully acknowledged.

References

[1] Stark, J.; Wicht, B. (2013) *Dauerhaftigkeit von Beton*. Springer Berlin Heidelberg, Berlin, Heidelberg.

[2] Crank, J. (1976) *The mathematics of diffusion*. 2. ed. Clarendon Press, Oxford.

[3] Timothy, J. J.; Meschke, G. (2016) *A micromechanics model for molecular diffusion in materials with complex pore structure*. International Journal for Numerical and Analytical Methods in Geomechanics 40, H. 5, pp. 686–712. https://doi.org/10.1002/nag.2423

[4] Dutzer, V. et al. (2019) *The link between gas diffusion and carbonation in hardened cement pastes*. Cement and Concrete Research 123, pp. 105–795. https://doi.org/10.1016/j.cemconres.2019.105795

[5] Leemann, A. et al. (2017) *Steady-state O2 and CO2 diffusion in carbonated mortars produced with blended cements*. Materials and Structures 50, H. 6. https://doi.org/10.1617/s11527-017-1118-3

[6] Sercombe, J. et al. (2007) *Experimental study of gas diffusion in cement paste*. Cement and Concrete Research 37, H. 4, pp. 579–588. https://doi.org/10.1016/j.cemconres.2006.12.003

[7] Boumaaza, M. et al. (2018) *A new test method to determine the gaseous oxygen diffusion coefficient of cement pastes as a function of hydration duration, microstructure, and relative humidity*. Materials and Structures 51, H. 2. https://doi.org/10.1617/s11527-018-1178-z

[8] Houst, Y. F.; Wittmann, F. H. (1994) *Influence of porosity and water content on the diffusivity of CO2 and O2 through hydrated cement paste*. Cement and Concrete Research 24, H. 6, pp. 1165–1176. https://doi.org/10.1016/0008-8846(94)90040-X

[9] Boumaaza, M. (2020) *Experimental Investigation of Gas diffusivity and CO2-Binding Capacity of Cementitious Materials* [Dissertation]. Technische Universität München. Universitätsbibliothek der TU München, München.

[10] Papadakis, V. G.; Vayenas, C. G.; Fardis, M. N. (1991) *Experimental investigation and mathematical modeling of the concrete carbonation problem*. Chemical Engineering Science 46, 5-6, pp. 1333–1338. https://doi.org/10.1016/0009-2509(91)85060-B

[11] Ngala, V. T.; Page, C. L. (1997) *Effects of carbonation on pore structure and diffusional properties of hydrated cement pastes*. Cement and Concrete Research 27, H. 7, pp. 995–1007. https://doi.org/10.1016/S0008-8846(97)00102-6

[12] Boumaaza, M. et al. (2020) *Influence of carbonation on the microstructure and the gas diffusivity of hardened cement pastes*. Construction and Building Materials 253, pp. 119–227. https://doi.org/10.1016/j.conbuildmat.2020.119227

[13] Yoon, I.-S. (2018) *Comprehensive Approach to Calculate Oxygen Diffusivity of Cementitious Materials Considering Carbonation*. International Journal of Concrete Structures and Materials 12, H. 1. https://doi.org/10.1186/s40069-018-0242-y

[14] Zhou, R. et al. (2021) *Assessment of Electrical Resistivity and Oxygen Diffusion Coefficient of Cementitious Materials from Microstructure Features*. Materials (Basel, Switzerland) 14, Nr. 12. https://doi.org/10.3390/ma14123141

[15] Villani, C. et al. (2014) *An inter lab comparison of gas transport testing procedures: Oxygen permeability and oxygen diffusivity*. Cement and Concrete Composites 53, pp. 357–366. https://doi.org/10.1016/j.cemconcomp.2014.05.004

[16] Marrero, T. R.; Mason, E. A. (1972) *Gaseous Diffusion Coefficients*. Journal of Physical and Chemical Reference Data 1, H. 1, pp. 3–118. https://doi.org/10.1063/1.3253094

[17] Guyer, J. E.; Wheeler, D.; Warren, J. A. (2009) *FiPy: Partial Differential Equations with Python*. Computing in Science & Engineering 11, H. 3, pp. 6–15. https://doi.org/10.1109/MCSE.2009.52

[18] DIN EN 197-1:2011-11 (2011) *Zement - Teil 1: Zusammensetzung, Anforderungen und Konformitätskriterien von Normalzement (EN 197-1:2011)*. Beuth Verlag GmbH, Berlin.

[19] Boumaaza, M. et al. (2018) *Gas diffusivity test method development: effect of cement paste saturation degree and concrete specimen thickness*. *'12th Fib International PhD Symposium in Civil Engineering' 2018, Proceedings of an international conference*. Czech Technical University, pp. 1087–1094.

[20] Christoforou, C. et al. (2021) *DIFCURV: A unified framework for Diffusion Curve Fitting and prediction in Online Social Networks*. Array 12, pp. 100. https://doi.org/10.1016/j.array.2021.100100

[21] Virtanen, P. et al. (2020) *SciPy 1.0: fundamental algorithms for scientific computing in Python*. Nature methods 17, Nr. 3, pp. 261–272. https://doi.org/10.1038/s41592-019-0686-2

[22] Wong, H. S.; Buenfeld, N. R.; Head, M. K. (2006) *Estimating transport properties of mortars using image analysis on backscattered electron images*. Cement and Concrete Research 36, H. 8, pp. 1556–1566. https://doi.org/10.1016/j.cemconres.2006.05.002

[23] Mezedur, M. M.; Kaviany, M.; Moore, W. (2002) *Effect of pore structure, randomness and size on effective mass diffusivity*. AIChE Journal 48, H. 1, pp. 15–24. https://doi.org/10.1002/aic.690480104